Track reconstruction for the *Mu3e* experiment based on a novel Multiple Scattering fit

Alexandr **Kozlinskiy**[1],[a] for the *Mu3e* Collaboration

[1]*Institut für Kernphysik, Johannes Gutenberg-Universität Mainz, Johann-Joachim-Becher-Weg 45, 55128 Mainz, Germany*

Abstract. The *Mu3e* experiment is designed to search for the lepton flavour violating decay $\mu^+ \to e^+e^+e^-$. The aim of the experiment is to reach a branching ratio sensitivity of 10^{-16}. In a first phase the experiment will be performed at an existing beam line at the Paul-Scherrer Institute (Switzerland) providing 10^8 muons per second, which will allow to reach a sensitivity of $2 \cdot 10^{-15}$. The muons with a momentum of about 28 MeV/c are stopped and decay at rest on a target. The decay products (positrons and electrons) with energies below 53 MeV are measured by a tracking detector consisting of two double layers of 50 μm thin silicon pixel sensors. The high granularity of the pixel detector with a pixel size of 80 μm × 80 μm allows for a precise track reconstruction in the high multiplicity environment of the *Mu3e* experiment, reaching 100 tracks per reconstruction frame of 50 ns in the final phase of the experiment. To deal with such high rates and combinatorics, the *Mu3e* track reconstruction uses a novel fit algorithm that in the simplest case takes into account only the multiple scattering, which allows for a fast online tracking on a GPU based filter farm. An implementation of the 3-dimensional multiple scattering fit based on hit triplets is described. The extension of the fit that takes into account energy losses and pixel size is used for offline track reconstruction. The algorithm and performance of the offline track reconstruction based on a full Geant4 simulation of the *Mu3e* detector are presented.

1 Introduction

The *Mu3e* experiment [2] is designed to search for Lepton Flavor Violation (LFV) in the decay $\mu^+ \to e^+e^+e^-$. The goal of the experiment is to observe this decay or set a limit on the branching fraction at the level of 10^{-16}. To reach such sensitivity, more than 10^{16} muon decays have to be observed and any backgrounds have to be suppressed to the 10^{-16} level. To achieve this goal within one year of data taking will require a muon stopping rate of more than 10^9 Hz with a high geometrical acceptance and efficiency of the detector.

In the Standard Mode (SM) lepton flavor is conserved at tree level. However, flavor is known to be not conserved in the neutrino sector where it is manifested in the form of neutrino oscillations. Contributions of neutrino mixing in loops however lead to an unobservable

---

[a]e-mail: akozlins@uni-mainz.de

branching fraction for $\mu^+ \to e^+e^+e^-$ of the order of 10^{-54} [1]. Consequently, the study of this decay is of large interest, as the observation of a signal will be a clear sign of New Physics (NP) beyond the Standard Model.

The current limit on the branching fraction of $\mu^+ \to e^+e^+e^-$ comes from the SINDRUM experiment and lies at $B(\mu^+ \to e^+e^+e^-) < 1.0 \cdot 10^{-12}$ at 90% CL [3]. *Mu3e* plans to improve this limit by four orders of magnitude.

The *Mu3e* experiment is planned to be performed in two phases. In the first phase the existing PiE5 beam line at the Paul-Scherrer Institute (PSI) will be used. During this phase the experimental concept and instrumentation will be validated. The goal for the first phase is to reach a sensitivity of $2 \cdot 10^{-15}$, improving the current limit by almost three orders of magnitude. For the second phase the installation of a new high intensity muon beam line (*HiMB*) is required, which has to provide a continuous beam of more than 10^9 muons per second.

1.1 Signal and background

The signal decay $\mu^+ \to e^+e^+e^-$ contains in the final state three particles: two positrons and one electron. The total momentum and energy of these three particles will correspond to the muon at rest ($\sum \boldsymbol{p} = 0$ and $\sum E = m_\mu$) as the muon stops and decays on target. In addition to the energy/momentum signature, the products of decay will have a common vertex and have to coincide in time.
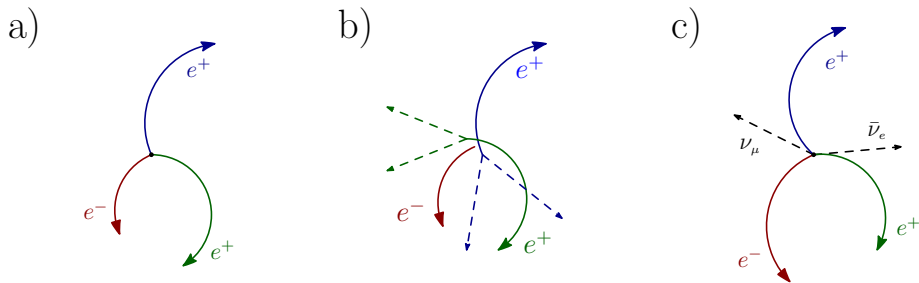
Figure 1. Schematic view of a) signal decay $\mu^+ \to e^+e^+e^-$, b) overlap of several Michel decays, c) internal conversion decay $\mu^+ \to e^+e^+e^-\nu\bar{\nu}$ where two neutrinos carry only part of the energy.

There are two sources of background. One is the combinatorial background due to several processes overlapping such that they mimic a signal decay, i.e. a positron from a Michel decay ($\mu^+ \to e^+\nu\bar{\nu}$) and an electron/positron pair from Bhabha scattering. Figure 1b shows a schematic view of such background. It can be suppressed with vertexing, good momentum and time resolution.

The second source is the internal conversion decay $\mu^+ \to e^+e^+e^-\nu\bar{\nu}$ where the only difference from the signal decay is missing energy and momentum. This type of background can only be suppressed with excellent momentum and energy resolution. Figure 2 shows the branching fraction of the internal conversion decay depending on the cut on missing energy [6]. At the level of 10^{-16}, the separation of signal and background is about 1.2 MeV, which requires a single particle momentum resolution of better than 0.5 MeV/c.
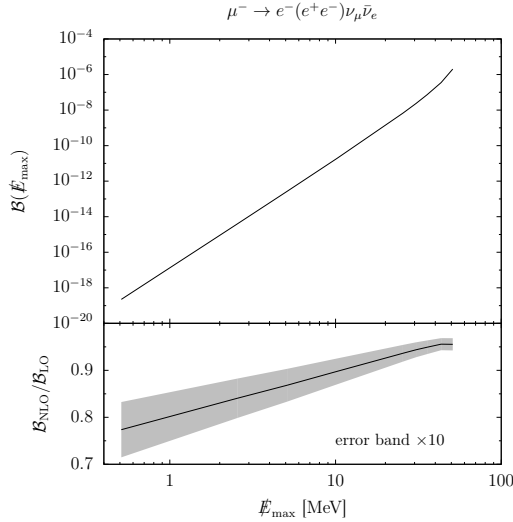
Figure 2. Branching fraction of decay $\mu^+ \to e^+ e^+ e^- \nu\bar{\nu}$ as function of cut on missing energy $\not{E} = m_\mu - E_{tot} < \not{E}_{max}$ [6]. At 10^{-16} level the cut lies at $\not{E}_{max} \approx 1.2$ MeV.

2 The *Mu3e* detector
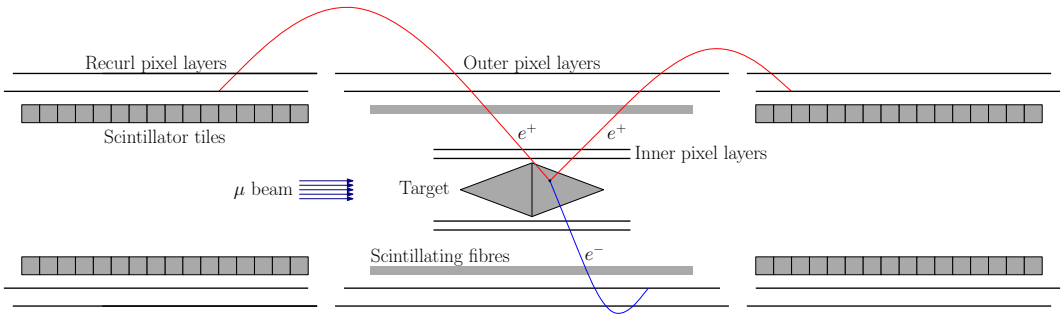
Figure 3. Schematic view of *Mu3e* detector cut open along beam line in the Phase I configuration. Not to scale.

The *Mu3e* detector has a design that is optimized for the detection of the $\mu^+ \to e^+ e^+ e^-$ signal decay. The whole detector is placed inside a 1 T solenoid magnet with 1 m bore and 2.5 m length. Figure 3 shows a schematic view of the phase I detector.

The muons with a momentum of about 28 MeV/c are stopped on a double cone hollow target and decay at rest. The target is made from 75 (85) μm of Mylar in the front (back) part and has a radius of 19 mm and length 100 mm which allows to spread vertices in space, reducing background due to random combinations of tracks and in addition helping to lower

the occupancy in the tracking detector. The products of the decays are detected by two double layers of silicon pixel sensors placed around the target. As the muon decays at rest, the maximum energy of the electrons/positrons produced is half the muon mass or about 53 MeV. Such low energies require to reduce as much as possible the amount of material seen by the particle, as multiple Coulomb scattering dominates the tracking uncertainty.

Mu3e will use High-Voltage Monolithic Active Pixel sensors (HV-MAPS [4]) that are based on a commercial HV-CMOS technology. These sensors can be thinned down to 50 μm which is less than 10^{-3} of a radiation length. All sensors of the tracker will have a size of 20×20 mm^2 with a pixel size of 80×80 μm^2. The sensors are mounted on a 25 μm kapton frame that provides mechanical support and a 50 μm Kapton/Aluminum readout flex print is used for power and signal routing.

The two inner layers consist of 8 and 10 ladders of six sensors and are placed as close as possible to the target to reduce the effect of multiple scattering and pixel size on the precision of the reconstructed vertex. The inner layers have a distance of about 23 mm and 29 mm respectively from the beam axis. The outer layers consist of 24 and 28 ladders of 18 sensors (total length of 36 cm) and have a distance to the beam axis of about 70 mm and 82 mm. The placement of the outer layer sets the limit on the minimum transverse momentum acceptance which is about 12 MeV/c.

Due to their low energy it is possible to measure particles when they bend back in the magnetic field. Such recurling particles will have better momentum resolution due to the constraint on the measured curvature (momentum) being limited only by the pixel size. To increase the acceptance for such recurling particles, two additional stations of double silicon layers are placed upstream and downstream of the central detector. The recurl stations have the same geometry as the outer double layers of the central station. The total length of the detector with recurl stations is about 1 m.

To further suppress accidental background, two timing detectors are used. Scintillating fibres are placed before the outer double layer of the central station and scintillating tiles are placed inside the recurl stations. The fibres of 28 cm length are arranged in ribbons that consist of three layers of 250 μm fibres and provide a time measurement with $\sigma_t \approx 0.5$ ns. The much thicker tiles will provide a time measurement for recurling tracks with $\sigma_t \approx 100$ ps.

The hit information will be readout continuously and assembled into 50 ns reconstruction frames. The data from all parts of the detector are collected by a readout system organized as a switching network consisting of FPGA boards and Gbit/s optical links. The combined data streams are routed to a filter farm where tracks and vertices are reconstructed.

3 Reconstruction

The reconstruction performance is studied on Monte Carlo (MC) data obtained with a full Geant4 simulation of the *Mu3e* detector. The simulated data are digitized and processed through the readout chain, where they are sorted and assembled to frames similar to real data. At 50 ns frame size and a muon stopping rate of $2 \cdot 10^8$ Hz there are about five Michel decays in each frame within the acceptance of the detector.

Each Michel positron produces on average two hits in each layer of the detector: one on the way out of the detector volume and another one when it recurls back. To identify tracks, it is necessary to find hits produced by the same particle and assemble them in the right order. In case of *Mu3e*, due to the low momentum, the hits from the same particle do not form straight segments and can be separated by large distances. This makes the identification

of tracks difficult and requires to consider many possible combinations of hits. As a minimum of three hits are necessary to define an initial trajectory or seed, the number of combinations that have to be processed or fitted scales as the third power of number of hits in a layer. For $n = 10$ the number of triplet candidate can reach 1000 per frame, which requires to be able to fit up to 10^{10} triplet candidates each second.

As it is not possible to store all the data produced by the detector, the online filter farm will be used to reduce the data rate by performing a full reconstruction of each frame [5]. To cope with such high rates and be able to fully reconstructed each frame *Mu3e* will use the novel 3-dimensional Multiple Scattering (MS) triplet fit [7].

3.1 Tripet fit

The triplet fit is designed for environments where the hit position uncertainties can be neglected compared to the multiple scattering. This is the case for the *Mu3e* experiment, where due to the low energies of particles multiple scattering dominates over other effects, such as pixel size.
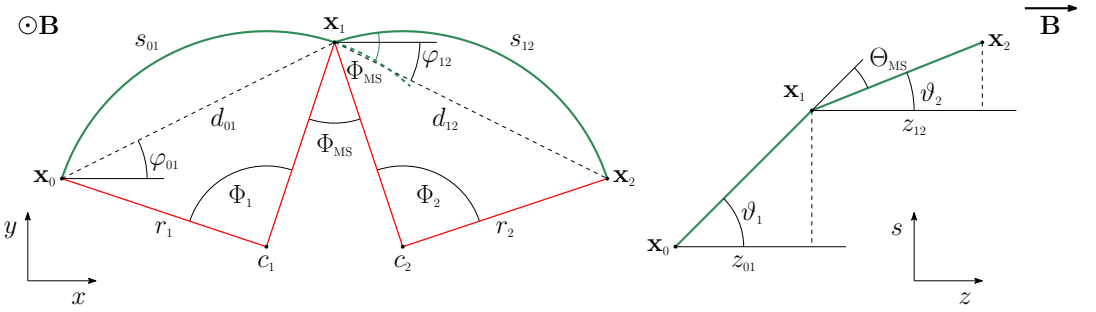
Figure 4. Schematic view of a triplet in the transverse (left) and longitudinal (right) plane. The green line shows a particle trajectory consisting of two helices between the hits x_0 and x_1, and x_1 and x_2. The scattering is defined at the middle hit x_1 with projected MS angles φ_{MS} and θ_{MS}.

The idea of the triplet fit comes from the fact that in the magnetic field the trajectory of the particle can be fully described by knowing the position of three hits (in 3D space) and the curvature (momentum), assuming negligible hit uncertainties and energy losses. In this scenario the trajectory consists of two helices between the first and second pair of hits and a kink at the middle hit, attributed to scattering, as shown in figure 4. The parameters of both helices are completely defined by the 3D curvature r of the trajectory. Consequently the scattering angle projections φ_{MS} and θ_{MS} are functions of r.

The fit can be defined as the trajectory that minimizes the total scattering angle or χ^2

$$\chi^2(r) = \varphi_{MS}^2(r)/\sin^2(\theta) + \theta_{MS}^2(r), \tag{1}$$

where θ is the helix polar angle.

The minimization problem is non-linear and does not have an analytic solution. However, the problem can be linearized around some known solution such that both φ_{MS} and θ_{MS} are linear functions of the curvature r. In case of small scattering angles, the initial solution can be selected as the trajectory that is circular in the transverse xy-plane. For this trajectory, the scattering angle in the transverse plane is zero and parameters of both helices can be

calculated from the positions of the hits. The solution to the minimization of the χ^2 in this linear case can be calculated [7].

In the case of tracks with more than three hits, the trajectory can be divided into a sequence of triplets such that each pair of triplets shares two hits. Due to the quadratic form of the triplet χ^2, it can be shown that the solution to the minimization of the track χ^2 is a weighted average of individual triplet solutions

$$r_{track} = \frac{\sum r_i \sigma_{r,i}^{-2}}{\sum \sigma_{r,i}^{-2}}, \tag{2}$$

where r_i and $\sigma_{r,i}$ are the curvature and uncertainty for triplet i.

The triplets can be fitted separately and subsequently combined together, however in practice the reconstruction starts with a seed triplet and additional hits are then added to the seed forming new triplets.

3.2 Track reconstruction

The reconstruction is performed in several steps. In a first step, the triplet seeds are formed which are subsequently used in the reconstruction of tracks. To reduce the number of triplet combinations, geometrical cuts on distances and opening angles between hits are used. After this, the triplets are fitted and a loose χ^2 cut is used to further reduce the number of wrong (fake) hit combinations. Still, the set of reconstructed triplets contains a large number of fakes, reaching 4 wrong for each truth matched combination.

Each triplet is then used as a seed for finding and reconstructing tracks that consist of at least 4 hits, with at least one hit in each layer. These are called short tracks and they correspond to the out- and in-going parts of the particle trajectory. For each triplet, the trajectory is extended to the outer layer and if there is a hit in the vicinity of the intersection of the layer with the trajectory, this hit is added to the triplet to form a short track. After the reconstruction of short tracks, the fake rate is reduced to the percent level. Figure 5a shows reconstructed triplets and short tracks in the transverse view of one reconstructed frame.

The short tracks are used for the reconstruction of recurling particles that form long tracks. There are two types of such tracks: 8- and 6- hits tracks. Long 8-hit tracks correspond to one full turn in the central part of the detector. Such tracks are reconstructed by combining two short tracks. Long 6-hit tracks are reconstructed from a short track and a pair of hits in two outer layers, either in the central or recurl stations. Figure 5b illustrates reconstructed long tracks in the transverse view of one reconstructed frame.

The fake rate for long 6-hit tracks is about 5%. For long 8-hit tracks the number of fakes can reach the number of truth tracks. Such a high fake rate is due to particles that make several turns in the magnetic field in the central part of the detector volume where wrong combinations are made from two short tracks that correspond to different turns.

For all types of track the fake rate due to the combination of hits from different tracks is of the order of 1%. The rest is coming from combinations of hits from the same track but different turns and can be reduced by applying cuts on the inclination angle of tracks, rejecting so-called vertical tracks.

In addition to random combinations, noise hits can contribute to the fake rate. Sensor noise is expected at a level of 0.1 Hz per pixel [8] which corresponds to about one noise hit per frame of 50 ns. At noise levels up to 10 Hz per pixel the contribution to the fake rate and the reconstruction efficiency is negligible.
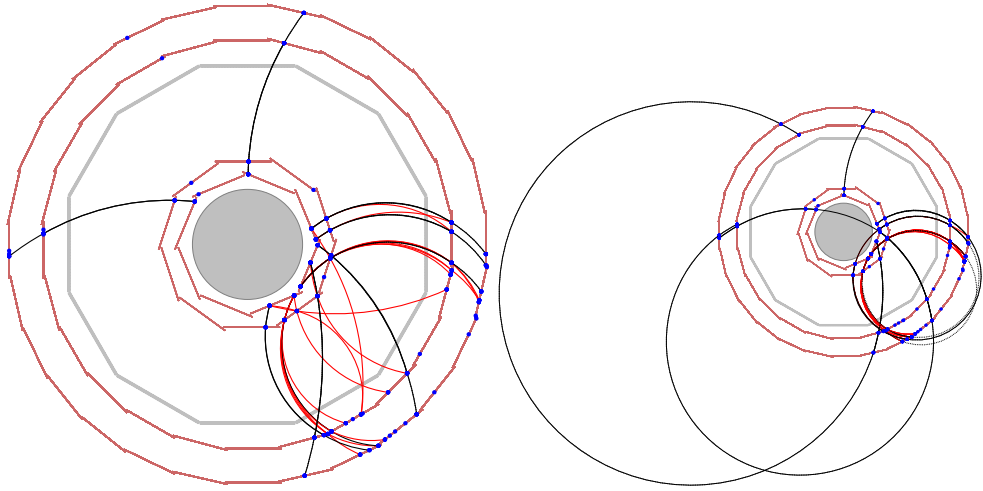
Figure 5. Transverse view of a reconstructed frame showing a) triplets and shorts tracks, b) long tracks. Truth matched and fake track candidates are shown in black and red respectively.

3.3 Performance

Figure 6 shows the total reconstruction efficiency (including acceptance) as a function of momentum p and inclination angle $\lambda = \pi/2 - \theta$.
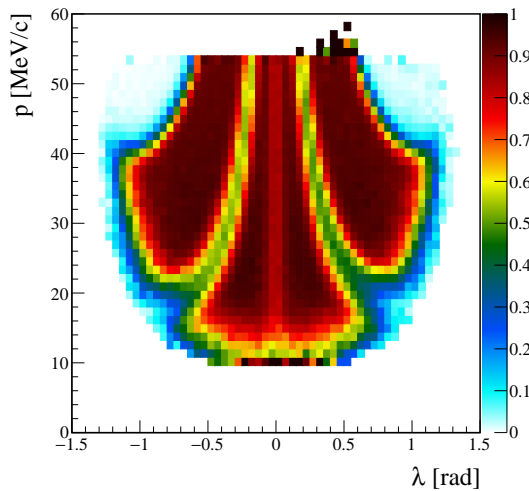
Figure 6. Total reconstruction efficiency for long tracks as a function of momentum p and inclination angle $\lambda = \pi/2 - \theta$. The edges of the distribution are defined by the geometry of the detector (radius of outer layer, length of the detector and gaps between stations).

The acceptance of the detector is limited by the outer radius of the detector which is represented by the lower edge in the efficiency plot. The missing corners are due to the limited length of the detector and vertical stripes correspond to service areas between the central and recurl stations. The efficiency is limited by geometrical cuts that are used to make the initial triplet seeds and by track χ^2 cuts.

The achieved momentum resolution for short and long tracks is shown in figure 7. The average momentum resolution for short tracks is $\sigma_p = 1.4$ MeV/c and for long tracks it is $\sigma_p = 0.2$ MeV/c.
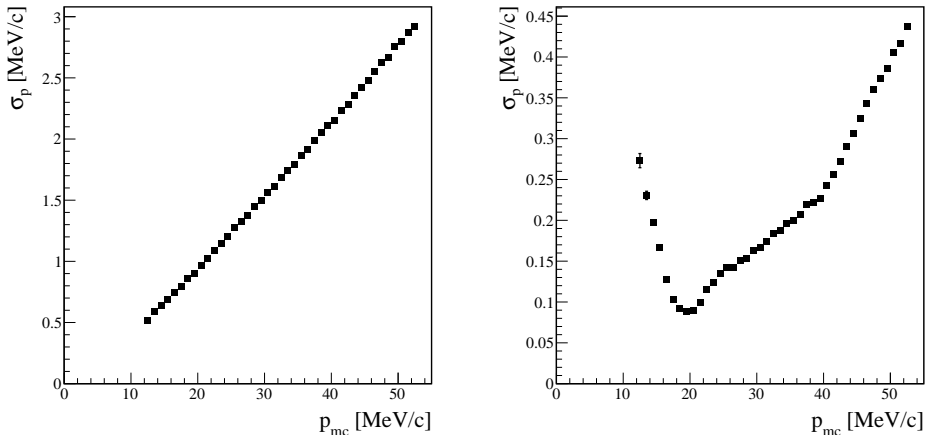
Figure 7. Momentum resolution for short (left) and long (right) tracks. The average momentum resolution is 1.4 MeV/c and 0.2 MeV/c respectively.

3.4 Charge ID

The timing information is provided by the fibre and tile detectors and is essential to reduce background due to random combinations of tracks. Each short track crosses the fibre detector and is assigned a fibre cluster. The long 8-hit tracks can have 2 fibre clusters, one for each short track.

The timing information is also used to resolve the charge ambiguity for reconstructed 8-hit long tracks. This ambiguity arises due to the unknown direction of motion of recurling particles. The fibre tracker allows to resolve the ambiguity by looking at the time difference between fibre hits. Figure 8 shows the time difference between two fibre hits as function of the corresponding path length. The positive time difference corresponds to right direction (charge) and negative time corresponds to the wrong charge id. The slope of the distribution corresponds to the speed of light.

3.5 Vertex fit and signal sensitivity

The final step of the reconstruction is the vertex fit. Three tracks from the signal decay should originate form a common point on the surface of the target. During the vertex fit, the
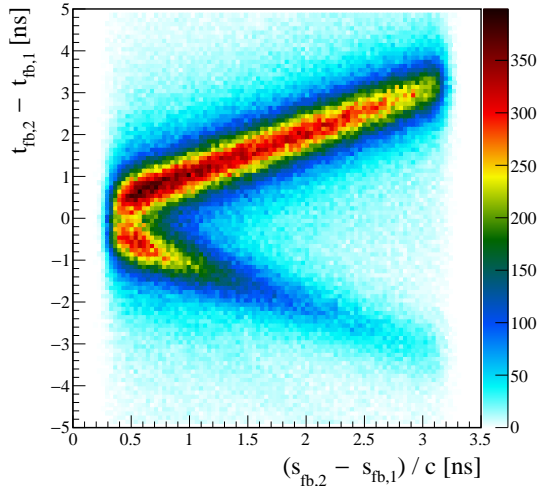
Figure 8. Distribution of the time difference between two fibre hits of recurling particle as a function of path length along the reconstructed trajectory from the first to the second fibre hit.

scattering in inner layers and the curvature uncertainties are taken into account. To suppress background, fit χ^2 and distance to target can be used. Figure 9 shows the distribution of distances between the reconstructed vertex and truth MC vertex position.

To estimate the signal sensitivity of the *Mu3e* experiment, simulated events with one signal decay in 50 ns reconstruction frame were generated. All combinations of two positively and one negatively charged tracks are tried to form a vertex that is fitted in the inner region of the detector. After the vertex fit, the invariant mass of the candidate signal decay is estimated from the parameters of the tracks at the vertex position. The reconstructed mass of candidates is shown in figure 9.

4 Summary

The *Mu3e* experiment is designed to search for the LFV decay $\mu^+ \to e^+ e^+ e^-$. The detector performance was studied with the full Geant4 detector simulation and reconstruction. In one year (10^7 seconds) of data taking with the muon stopping rate of $2 \cdot 10^8$ Hz on target *Mu3e* will be able to reach a single event sensitivity at the $2 \cdot 10^{-15}$ level. This corresponds to the target sensitivity of the first phase of the experiment. The current detector design is shown to reach and exceed the sensitivity requirements in terms of momentum and invariant mass resolution.

References

[1] W. J. Marciano, T. Mori and J. M. Roney, "Charged Lepton Flavor Violation Experiments," Ann. Rev. Nucl. Part. Sci. **58** (2008) 315. doi:10.1146/annurev.nucl.58.110707.171126
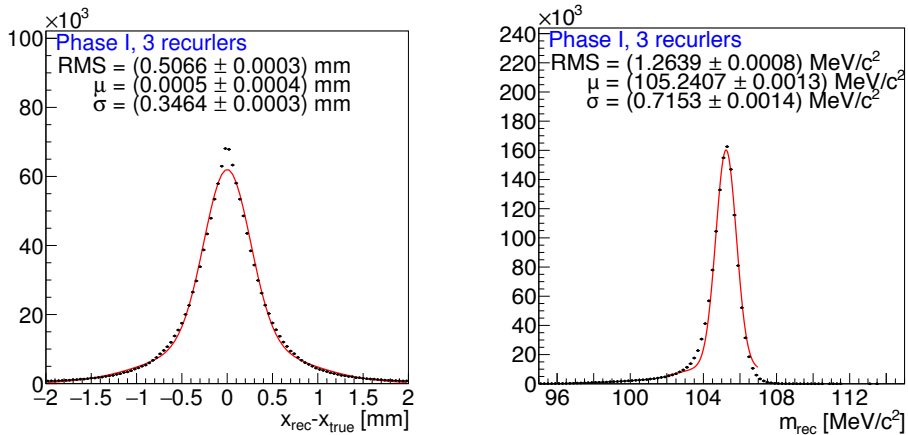
Figure 9. Distance from truth vertex position x_{true} to the reconstructed vertex x_{rec} (left) and invariant mass distribution of truth candidates.

[2] A. Blondel, A. Bravar, M. Pohl, S. Bachmann, N. Berger, M. Kiehn, A. Schoning and D. Wiedner *et al.*, "Research Proposal for an Experiment to Search for the Decay $\mu^+ \to e^+e^+e^-$," arXiv:1301.6113 [physics.ins-det].

[3] U. Bellgardt *et al.* [SINDRUM Collaboration], "Search for the Decay $\mu^+ \to e^+e^+e^-$," Nucl. Phys. B **299**, 1 (1988).

[4] I. Peric, "A novel monolithic pixelated particle detector implemented in high-voltage CMOS technology," Nucl. Instrum. Meth. A **582**, 876 (2007).

[5] D. vom Bruch, "Online Track and Vertex Reconstruction on GPUs for the Mu3e Experiment," Workshop "Connecting The Dots / Intelligent Trackers 2017", LAL-Orsay.

[6] M. Fael and C. Greub, "Next-to-leading order prediction for the decay $\mu \to e\ (e^+e^-)\ \nu\ \bar{\nu}$," JHEP **1701** (2017) 084 doi:10.1007/JHEP01(2017)084 [arXiv:1611.03726 [hep-ph]].

[7] N. Berger, M. Kiehn, A. Kozlinskiy and A. Schöning, "A New Three-Dimensional Track Fit with Multiple Scattering," Nucl. Instrum. Meth. C **844** (2017) 135 doi:10.1016/j.nima.2016.11.012 [arXiv:1606.04990 [physics.ins-det]].

[8] H. Augustin *et al.*, JINST **11** (2016) no.11, C11029 doi:10.1088/1748-0221/11/11/C11029 [arXiv:1610.02210 [physics.ins-det]].